Am J Cancer Res 2020;10(7):2145-2159
www.ajcr.us /ISSN:2156-6976/ajcr0116581

*Original Article*

# Comparison of the amino acid profile between the nontumor and tumor regions in patients with lung cancer

Haruka Namikawa-Kanai[1,2], Teruo Miyazaki[3], Taisuke Matsubara[1], Shunsuke Shigefuku[1], Shotaro Ono[2], Eiji Nakajima[2], Yukio Morishita[4], Akira Honda[3,5], Kinya Furukawa[2], Norihiko Ikeda[1]

*[1]Department of Surgery, Tokyo Medical University, Tokyo, Japan; [2]Department of Thoracic Surgery, [3]Joint Research Center, [4]Diagnostic Pathology Division, Tokyo Medical University Ibaraki Medical Center, Ibaraki, Japan; [5]Department of Internal Medicine, Division of Gastroenterology and Hepatology, Tokyo Medical University Ibaraki Medical Center, Ibaraki, Japan*

Received June 19, 2020; Accepted June 27, 2020; Epub July 1, 2020; Published July 15, 2020

**Abstract:** Energy metabolism in cancer cells is reprogrammed to meet the energy demands for cell proliferation under strict environments. In addition to the specifically activated metabolism of cancer, including the Warburg effect and glutaminolysis, most amino acids (AAs) are utilized for gluconeogenesis. Significant increases in AAs and energy metabolites in the tumor region occur in gastric and colon cancers. However, a different AA-related energy metabolism may exist in lung cancer because of the abundant blood supply to lung tissue. This study compared the profiles of AAs and their related metabolites in energy metabolism, analyzed by an HPLC-MS/MS system, between tissues from nontumor and tumor regions collected from 14 patients with non-small cell lung cancer (NSCLC). In the energic metabolism precursor categories, the glucogenic AAs, which included the pyruvate precursors (Ser, Gly, Thr, Ala, and Trp), the α-ketoglutarate precursors (Glu, Gln, and Pro) and the succinyl-CoA precursors (Val, Ile, and Met) were significantly increased in the tumor region compared to in the nontumor region. However, no significant differences existed between the two regions in the ketogenic AAs (Leu, Lys, and Tyr). These differences were not observed between the subgroups with and without diabetes mellitus in the two regions. The metabolites on the left-hand side of the TCA cycle were significantly higher in the tumor region, but no differences in metabolites in the right-hand side. The mRNA expressions of major AA transporters and cancer proliferation factors were also significantly increased in the tumor region, compared to these in their counterparts. In lung cancer, glucogenic AAs that are actively transported from circulating fluids would be predominantly utilized for gluconeogenesis, with and without diabetes mellitus. The characteristics of the AA-related metabolism would be associated with tissue-specific cell proliferation in patients with NSCLC.

**Keywords:** NSCLS, amino acids, tumor region, energy metabolism, gluconeogenesis

## Introduction

Cancer cells have to reprogram specific energy metabolism to meet increased energetic demands for cell growth in strict environments such as hypoxia and nutrient-restrictive conditions [1], and favor anaerobic glucose utilization, which is called the “Warburg’s effect” [2]. In addition, two mitochondrial anaplerotic pathways involving the gluconeogenesis via pyruvate carboxylation and glutamine breakdown, called as “glutaminolysis”, are also required as alternative energetic metabolism for cancer cell growth [3-6]. In addition to glutaminolysis, most amino acids (AAs) are utilized in the cancer cells for the intermediate precursors in energy metabolism. The comprehensive free AA profiling in a blood sample, called Amino Index Cancer Screening, based on the organ-specific differences, has practical use for the early screening of six types of cancer: lung, gastric, colorectal, breast, prostate, and uterine/cervical cancers [7-9]. The reason for the characteristics of blood AAs of cancer patients may be, at least partially, because cancer cells utilize AAs for energy production in the cancer cells.

In the colon and stomach cancers, the significant accumulations of most kinds of AAs, except for glutamine, in the tumor region, compared to in the paired nontumor region, collected from the same patient have been reported by using quantitative metabolome analysis with capillary electrophoresis time-of-flight mass spectrometry [10]. The cancer-specific characteristics in gastrointestinal organs suggested enhanced energy metabolism, as well as autophagic protein degradation.

Imbalances in AAs have been observed in the blood of the patients with lung cancer [9, 11]; therefore, similar cancer-specific metabolism that involves AAs may also be enhanced in the tumor region of lung tissue. However, the environments surrounding cancers in the lung in where is exposed to a higher level of oxygen, are distinctive, compared to the different cancer types. Milne [12] demonstrated the presence of a dual blood supply from the pulmonary and the bronchial artery systems in lung tumors. Therefore, lung cancer cells may exist in different environments from hypoxic to a low nutrient states where other types of cancer exist and thus have their own specific energy metabolism involved AAs.

We hypothesized that AA metabolism involved in energy production, including glutaminolysis, would be altered in lung cancer cells, compared to the noncancer (i.e., normal) cells. The aim of the present study was to compare the profiles of AAs and their related metabolites between the tumor and the paired nontumor regions resected from lung tissue in patients with non-small-cell lung cancer (NSCLC).

## Methods

### *Subjects and sample collection*

Fourteen patients with NSCLC (69.6 ± 2.8 years old [mean ± standard error]; male:female ratio = 7:7) who underwent surgical lung resection from January 2018 to January 2019 in Tokyo Medical University Ibaraki Medical Center (Ibaraki, Japan) were enrolled for the present study. The NSCLC types were adenocarcinoma (7 cases), squamous cell carcinoma (6 cases), and pleomorphic carcinoma (1 case). The lung cancer stages were IA1 (3 cases), IA2 (2 cases), IA3 (2 cases), IB (3 cases), IIA (3 cases), and IIIA (1 case). Five patients were diagnosed with type II diabetes mellitus (T2DM). The blood glucose levels in the subgroups without T2DM and with T2DM were 91.4 ± 4.9 mg/dL and 117.8 ± 6.2 mg/dL, respectively ($P$<0.01).

Tumor and nontumor regions were collected from the remaining lung tissue, after collection for histological diagnosis. The tumor and nontumor tissues were evaluated by pathologists. The nontumor region was collected from the margin region far from the tumor tissue by avoiding around the tumor tissue. The collected tissues were immediately frozen and stored at -80°C until analyses.

The methods and purpose of the study were explained to the patients, and their informed consent was obtained before enrollment. The study protocol was approved by the Ethics Committee of Tokyo Medical University Ibaraki Medical Center (approval no. 17-21) and was conducted in accordance with the 1964 Helsinki declaration.

### *Sample preparation for biochemical analyses*

In the first step for analysis, nontumor tissue that was attached to the tumor region was carefully removed, and the center part in the tumor tissue was removed as the tumor region for analysis. Fifty milligrams wet weight of both regions were washed several times with ice-cold PBS until the adhered blood was completely removed. The tissue was sonicated with 10-times volume (*w/v*) of PBS, and centrifugated at 3,500 × *g* for 10 minutes, 4°C. The supernatant was collected and used for biochemical analyses of organic acids, glucose, lipids, and protein. Glucose, triglyceride, total cholesterol, and total protein levels in both regions were measured in the supernatant by using commercially available assay kits (Glucose CII-test Wako, Cholesterol E-test Wako, Triglyceride E-test Wako [all by FUJIFILM Wako Pure Chemical Corporation, Osaka, Japan] and Pierce BCA Protein Assay Kit [Thermo Fischer Scientific, Waltham, MA, USA], respectively). The levels of glucose, lipids and organic acids in the nontumor and tumor regions are presented as per total-protein.

### *Amino acids analysis*

Amino acid concentrations in the supernatants obtained from the tumor and nontumor regions

in the lung were quantified by using a derivatization method with 3-aminopyridyl-N-hydroxysuccinimidyl carbamate (APDS) [13, 14] using a high-performance liquid chromatography electrospray ionization tandem mass spectrometry (HPLC-ESI-MS/MS) system consisting of the TSQ Vantage triple stage quadruple mass spectrometer (Thermo Fisher Scientific) equipped with an HESI-II probe and a Prominence ultrafast liquid chromatography system (Shimadzu, Kyoto, Japan).

The sample supernatant was mixed with 50 µL of APDSTAG® Wako Amino Acids Internal Standard (IS) Mixture solution (FUJIFILM Wako Pure Chemical Corporation) and 100 µL of acetonitrile and centrifuged at 20,000 × *g* for 10 minutes. Twenty microliters of the APDS-acetonitrile solution (20 mg/mL; FUJIFILM Wako Pure Chemical Corporation) and 60 µL of 0.2 M sodium borate buffer at *pH* 8.8 were mixed with 20 µL of the supernatant and incubated at 55°C for 10 minutes. The reaction mixture was thereafter added to 100 µL of 0.1% formic acid solution. Five microliters were injected into the LC-P-ESI-MS/MS system. Amino Acids Mixture Standard solutions of Type B and AN-2 (FUJIFILM Wako Pure Chemical Corporation) were used for quantification. The APDS-derivatized amino acids were separated using the 100 × 2.0 mm i.d. Wakosil-II $^{3}C_{8}$-100HG column (particle size 3 µm) as the analytical column and the 10 × 1.5 mm i.d. Wakosil-II $^{3}C_{8}$-100HG column as the guard column (particle size 3 µm) (FUJIFILM Wako Pure Chemical Corporation) at a gradient flow of 0.3 mL/min at 40°C. The general HPLC and MS/MS conditions were conducted by using a previously reported method [13].

*Analyses of pyruvate and TCA cycle metabolites*

Pyruvate and TCA cycle metabolites such as citrate, isocitrate, α-ketoglutarate, succinate, fumarate, and malate were measured with HPLC-ESI-MS/MS system, based on methods described previously [15]. Fifty microliters of the tissue supernatants were mixed with 934 pmol (100 ng) of [$^{13}C_{3}$] malonate (FUJIFILM Wako Pure Chemical Corporation) as the IS in 200 µL of acetonitrile. After centrifugation at 2,000 × *g* for 1 minute, the liquid phase was collected and evaporated to dryness at 55°C under a nitrogen stream. The residue was redissolved in 30 µL of water and centrifuged again at 2,000 × *g* for 1 minute. The supernatants were collected and a 5 µL of aliquot was injected into the HPLC-ESI-MS/MS system.

Chromatographic separation was performed using the Hypersil GOLD a Q column (150 × 2.1 mm, 3 µm, Thermo Fisher Scientific) at 40°C. The mobile phase was composed of methanol-water (1:19, *v/v*) containing 0.1% formic acid, and was used at a flow rate of 300 µL/min. The MS/MS conditions were as follows: spray voltage, 2500 V; vaporizer temperature, 450°C; sheath gas (nitrogen) pressure, 50 psi; auxiliary gas (nitrogen) flow, 15 arbitrary units; ion transfer capillary temperature, 220°C; collision gas (argon) pressure, 1.0 motor; ion polarity, negative; and selected reaction monitoring (SRM) and collision energy, *m/z* 106 → *m/z* 61 (13 V) for [$^{13}C_{3}$]malonate, *m/z* 115 → *m/z* 71 (13 V) for fumarate, m/z 117 → *m/z* 73 (17 V) for succinate, *m/z* 133 → *m/z* 115 (15 V) for malate, *m/z* 145 → *m/z* 101 (12 V) for α-ketoglutarate, *m/z* 191 → *m/z* 87 (18 V) for citrate, and *m/z* 191 → *m/z* 155 (15 V) for isocitrate.

*Analyses of hydroxybutyrates and lactate*

2-hydroxybutyrate (2HB), 3-hydroxyisobutyrate (3HIB), and lactate were measured with derivatization into 2-pyridinemethanol (2PM) esters, based on a method described previously [16]. The derivatization of hydroxybutyrates into 2PM esters was conducted with some modifications, based on a previous method for the synthesis of carboxylic esters [17]. Five microliters of the supernatant were mixed with 100 ng of sodium DL-3-hydroxyisobutyrate-$^{13}C_{4}$ ([$^{13}C_{4}$]3HB; Merck KGaA, Darmstadt, Germany) in 100 µL and 500 ng of DL-lactate-[$^{2}H_{3}$] (lactate-d3; C/D/N Isotopes Inc. Quebec, Canada) of acetonitrile-water (19:1, *v/v*) as the ISs.

After undergoing the aforementioned centrifugation and evaporation steps, the residue was incubated with 50 µL of freshly prepared reagent mixture consisted of 2-methyl-6-nitrobenzoic anhydride (3.35 mg), 4-dimethylaminopyridine (4 mg), pyridine (45 µL) and 2-pyridinemethanol (5 µL) at room temperature for 30 minutes. The reaction reagent was added to 1 mL of diethyl ether and centrifuged at 700 × *g* for 1 minute. The collected clear supernatant

was evaporated at 55°C under nitrogen and then redissolved in 100 μL of 0.1% formic acid in water. After centrifugation at 700 × *g* for 1 minute, the supernatant was collected. A 5 μL of aliquot was injected into the HPLC-MS/MS system.

Chromatographic separation was performed by using the Hypersil GOLD a Q column (Thermo Fisher Scientific) at 40°C. The mobile phase was initially acetonitrile-water (1:19, *v/v*) containing 0.2% formic acid. It was used at a flow rate of 300 μL/min for 5 minutes. After 5 minutes, the mobile phase was switched to 0.2% formic acid in acetonitrile at a flow rate of 300 μL/min for an additional 7 minutes. The general MS/MS conditions were as follows: spray voltage, 3000 V; vaporizer temperature, 450°C; sheath gas (nitrogen) pressure, 50 psi; auxiliary gas (nitrogen) flow, 15 arbitrary units; ion transfer capillary temperature, 220°C; collision gas (argon) pressure, 1.0 mTorr; collision energy, 15 V; and ion polarity, positive; and SRM, *m/z* 196 → *m/z* 110 for the 2PM-2HB and 2PM-3HIB, *m/z* 200 → *m/z* 110 for the 2PM-[$^{13}C_4$]3HB, *m/z* 182.1 → *m/z* 110.1 for the 2PM-Lactate, and *m/z* 185.1 → *m/z* 110.1 for the 2PM-Lactate-d3.

*Total RNA extraction and PCR analysis*

One hundred milligram wet weight of the tumor and nontumor tissues were homogenized with a 10-times volume of lysis buffer. The total RNA was extracted using the RNeasy Plus Mini Kit (QIAGEN K.K., Tokyo, Japan). Reverse transcription was conducted on 0.5 μg of total RNA by using the PrimeScript RT reagent Kit (TAKARA Bio. Inc., Shiga, Japan). Real-time quantitative PCR was conducted on cDNA aliquots with the FastStart DNA Master SYBR Green I and the LightCycler (Roche Diagnostics, Mannheim, Germany). The sequences of the oligonucleotide primer pairs used to amplify the mRNA are shown in **Table 1**.

The PCR amplification began with a 10-minute preincubation step at 95°C, followed by 40 cycles of denaturation at 95°C for 10 seconds, annealing at 62°C for 10 seconds, and elongation at 72°C. The relative concentration of PCR products derived from the target gene was calculated using LightCycler System software (Roche Diagnostics).

A standard curve for each run was constructed by plotting the crossover point against the log concentration. The concentration of target molecules in each sample was calculated automatically by reference to this curve (r = -1.00). The results were standardized to the expression of 18SrRNA. The specificity of each PCR product was assessed by melting curve analysis.

*Statistical analyses*

Data are presented as mean ± the standard error. Statistical differences between the tumor and paired nontumor regions, and statistical differences between the patient groups with and without T2DM in the sub-comparison analysis were analyzed by using the paired Student's *t*-test and the repeated two-way two-way analysis of variance multiple comparison test, respectively. A value of $P<0.05$ was significant. Statistics were analyzed using Prism software (version 7, GraphPad Software Inc., San Diego, CA).

## Results

*Amino acid levels in the tumor and nontumor regions*

The tissue levels of AAs in the tumor and nontumor regions in the lung are shown in the scheme in energy metabolic pathway in **Figure 1**. The examined AAs were categorized as glucogenic AAs and ketogenic AAs. The former category was further divided into pyruvate precursors, α-ketoglutamate precursors, and succinyl-CoA precursors. The latter category consisted of acetyl-CoA precursors. The levels of all AAs in the glucogenic AAs, except for Cys and Arg, were significantly higher in the tumor region than in the nontumor region. No significant difference existed between the two regions in Cys and Arg levels. The sums of AAs in the pyruvate, α-ketoglutamate, and succinyl-CoA precursors were also significantly higher in the tumor region than in the paired nontumor region (**Figure 2**). In the metabolites from the succinyl-CoA precursors, 3HIB, which is an intermediate of valine, and 2HB, which is a byproduct of methionine and threonine through 2-ketobutyrate were also significantly higher in the tumor region than in the nontumor region (**Figure 1**).

In the ketogenic AAs, no significant difference existed in lysine, leucine, and tyrosine levels between the two regions, but phenylalanine, the precursor of tyrosine, was significantly high-

**Table 1.** Gene sequences of PCR primers

| Gene | Accession number | | Sequence | Product Size (*bp*) |
|---|---|---|---|---|
| 18SrRNA | X03205 | F | GTAACCCGTTGAACCCCATT | 151 |
| | | R | CCATCCAATCGGTAGTAGCG | |
| β-actin | NM_001101 | F | ACTGGGACGACATGGAGAAA | 189 |
| | | R | ATAGCACAGCCTGGATAGCA | |
| ASCT2 | NM_005628 | F | TCCTCTTCACCCGCAAAAACCC | 134 |
| | | R | CCACGCCATTATTCTCCTCCAC | |
| $ATB^{0,+}$ | NM_007231 | F | TGACCACTTCTGTGCTGGATGG | 155 |
| | | R | AGCAAGCTCTCCACCATAGCCA | |
| BCAT2 | NM_001190 | F | CGCTGAATGGTGTTATCCTG | 109 |
| | | R | AACTGCTTCATGGTGATCGT | |
| cMyc | NM_002467 | F | CCTGGTGCTCCATGAGGAGAC | 128 |
| | | R | CAGACTCTGACCTTTTGCCAGG | |
| GLS1 | NM_001256310 | F | CAGAAGGCACAGACATGGTTGG | 117 |
| | | R | GGCAGAAACCACCATTAGCCAG | |
| GLUT1 | NM_006516 | F | CTGCAACGGCTTAGACTTCGAC | 101 |
| | | R | TCTCTGGGTAACAGGGATCAAACA | |
| GLUT3 | NM_006931 | F | TGCCTTTGGCACTCTCAACCAG | 98 |
| | | R | GCCATAGCTCTTCAGACCCAAG | |
| HIF-1α | NM_001243084 | F | TATGAGCCAGAAGAACTTTTAGGC | 145 |
| | | R | CACCTCTTTTGGCAAGCATCCTG | |
| HIF-1β | NM_001197325 | F | CTGTCATCCTGAAGACCAGCAG | 129 |
| | | R | CTGGTTCTCATCCAGAGCCATTC | |
| LAT1 | NM_003486 | F | GCCACAGAAAGCCTGAGCTTGA | 136 |
| | | R | ATGGTGAAGCCGATGCCACACT | |
| LAT3 | NM_003627 | F | ATGGACTGGCGGATCAAGG | 109 |
| | | R | TCTTGCAGTAGCGTGGTCTGATG | |
| MCT1 | NM_003051 | F | TGGCACCAGGCAAACGAATA | 137 |
| | | R | AAATGCATCCAGCAATTCTAAGCAC | |
| MCT2 | NM_001270623 | F | CCTGCGCCAGAGACCAGATAA | 109 |
| | | R | TTGGCACCAAGAGTCCCAGAG | |
| PCK1 | NM_002591 | F | TGGATGAAGTTTGACGCACA | 124 |
| | | R | TGTTCTTCTGGATGGTCTTGAT | |
| PCK2 | NM_004563 | F | TGACGCCATCATCTTTGGTG | 163 |
| | | R | CATGGCAAATGGGTCGTG | |
| VEGFα | NM_001025366 | F | TTGCCTTGCTGCTCTACCTCCA | 126 |
| | | R | GATGGCAGTAGCTGCGCTGATA | |
| xCT | NM_014331 | F | TCCTGCTTTGGCTCCATGAACG | 122 |
| | | R | AGAGGAGTGTGCTTGCGGACAT | |

*18SrRNA*, 18S ribosomal RNA; *ASCT2*, system ASC transporter 2 (SLC1A5); $ATB^{0,+}$, amino acid transporter responsible for the activity of system $B^{0,+}$ (SLC6A14); *BCAT2*, branched chain amino acid transaminase-2; *cMYC*, MYC proto-oncogene (bHLH transcription factor); *GLS1*, glutaminase 1; *GLUT3,* glucose transporter subtype 3 (SLC2A3); *HIF-1α & β*, hypoxia-inducible factor-1*α* & *β*; *LAT1 & 3*, L-type amino acid transporter 1 & 3 (SLC7A5 & SLC43A1); *MCT1, 2, & 4*, monocarboxylate transporter (SLC16A1, SLC16A7, & SLC16A4); *PCK1*, phosphoenolpyruvate carboxykinase 1; *VEGFα*, vascular endothelial growth factor *α*; *xCT*, system $x_c^-$ transporter-related protein (SLC7A11); *F*, forward; *R*, reverse; *bp*, base pair.

er in the tumor region than in the nontumor region (**Figure 1**). The sum of the ketogenic AAs was not significantly different between the two regions (**Figure 2**).

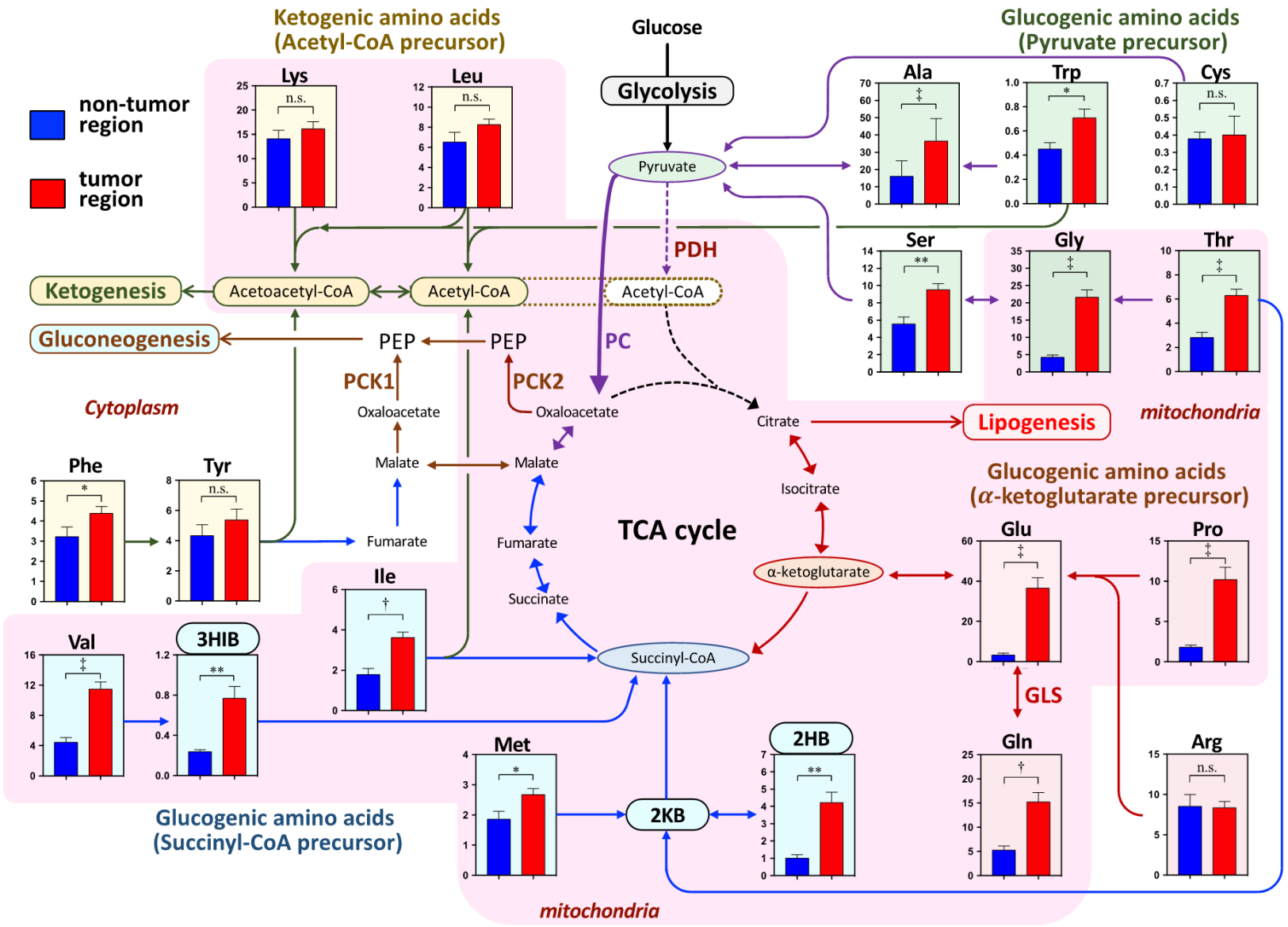


**Figure 1.** The scheme of the amino acid (AA)-related energy metabolic pathway shows the amino acids and their metabolites in the nontumor and tumor regions. Amino acids are categorized as ketogenic AAs or glucogenic AAs, based on their metabolic precursors. The former group consists of the precursors of common acetyl-CoA or acetoacetyl-CoA. The latter group is further subdivided into the precursors of pyruvate, α-ketoglutamate, succinyl-CoA, fumarate, and malate. Some

AAs belong to both categories, but in the present study, the ketogenic AAs are Phe, Try, Lys, and Leu; the pyruvate precursor AAs are Ser, Gly, Thr, Ala, Trp, and Cys; the α-ketoglutamate precursor AAs are Pro, Arg, Glu, and Gln; the succinyl-CoA precursor AAs are Val, Ile, Met, and Thr. The AA-related energy metabolism occurs in the mitochondria, which have a pink background, and in the cytoplasm, which has an uncolored background. The concentrations of AAs and metabolites are presented by the tissue total protein level (nmol/mg total protein) and as the mean ± the standard error. **P*<0.05, ***P*<0.01, †*P*<0.001, and ‡*P*<0.0001 indicate the significant difference levels, analyzed using the paired Student's *t*-test. Abbreviation: 2KB, 2-ketobutyrate; 2HB, 2-hydroxybutyrate; 3HIB, 3-hydroxyisobutyrate; AA, amino acid; GLS, glutaminase; PC, pyruvate carboxylase; PEP, phosphoenolpyruvate; PCK1 & PCK2, phosphoenolpyruvate carboxykinase 1 (cytoplasm) & 2 (mitochondria).

Significant differences in AA levels between the two regions were also detected when patients were divided into the with T2DM and without T2DM groups (**Table 2**). However, the AA levels in the tumor and nontumor regions were not significantly different between the with T2DM and without T2DM groups (**Table 2**).

*The metabolite levels in the AA-involved energic production pathways*

Accompanied by the significant increases of the pyruvate precursor AAs, pyruvate and its metabolite lactate in the glycolysis pathway were significantly higher in the tumor region than in the nontumor region (**Figure 2**). In addition, the glucose level was also significantly higher in the tumor region than the nontumor region (**Figure 2**). However, no significant differences existed in the glucose level between the two regions in the patients with and without T2DM (**Table 2**).

The α-ketoglutamate precursor AAs (i.e., glutamate, glutamine, and proline) were significantly higher in the tumor region. However, the right-hand side metabolites (e.g., citrate, isocitrate, and α-ketoglutamate) of the TCA cycle were not significantly different between the two regions (**Figure 2**). In addition, the triglyceride level in the tumor region was similar to that in the nontumor region (**Figure 2**). However, on the left-hand side of the TCA cycle, the metabolite levels of malate, fumarate, and succinate were significantly increased in the tumor region, compared to their levels in the nontumor region, accompanied by significant increases in the Succinyl-CoA precursor AAs (**Figure 2**).

*mRNA expressions of enzymes, transporters, and cancer factors*

**Figure 3A-C** show the mRNA expression levels of transporters, enzymes, and cancer proliferative factors in both regions. For the major AA transporters, the mRNA expressions of L-type AA transporter isoform 1 and 3 (SLC7A5 and SLC43A1; LAT1 and LAT3), system ASC transporter 2 (SLC1A5; ASCT2), and system $x_c^-$ transporter-related protein (SLC7A11; xCT) were significantly increased in the tumor region, compared to their levels in the nontumor region (**Figure 3A**). The expression level of the AA transporter responsible for the activity of system $B^{0,+}$ (SLC6A14; $ATB^{0,+}$) mRNA was also increased, but not significantly so, in the tumor region.

For the glucose transporters, the subtype 1 (SLC2A1; Glut1) mRNA expression was significantly increased in the tumor region, compared to its expression in the nontumor region, but mRNA expression of subtype 3 (SLC2A3; Glut3) was not significantly different between the nontumor and tumor regions (**Figure 3A**). The mRNA expressions of monocarboxylate transporter subtype 1 and 2, which import extracellular lactate (SLC16A1 & SLC16A7; MCT1 & MCT2), were significantly higher in the tumor region than in the counterparts (**Figure 3A**).

Among the phosphoenolpyruvate carboxykinase (PEPCK) genes, the mRNA expressions of cytoplasm and mitochondrial isoforms (PCK1 and PCK2, respectively) were significantly lower and higher, respectively, in the tumor region than in the nontumor region (**Figure 3B**). In the AA metabolic enzymes, the mRNA expression levels of glutaminase 1 (GLS1), which metabolizes glutamine to glutamate, and branched-chain amino acid transaminase-2 (BCAT2), which deaminates valine, leucine, and isoleucine, were significantly higher in the tumor region than in the nontumor region.

In the tumor region, the mRNA levels of all examined cancer cell proliferative factors such as MYC proto-oncogene (a basic helix-loop-helix transcription factor), vascular endothelial growth factor α (VEGFα), hypoxia-inducible

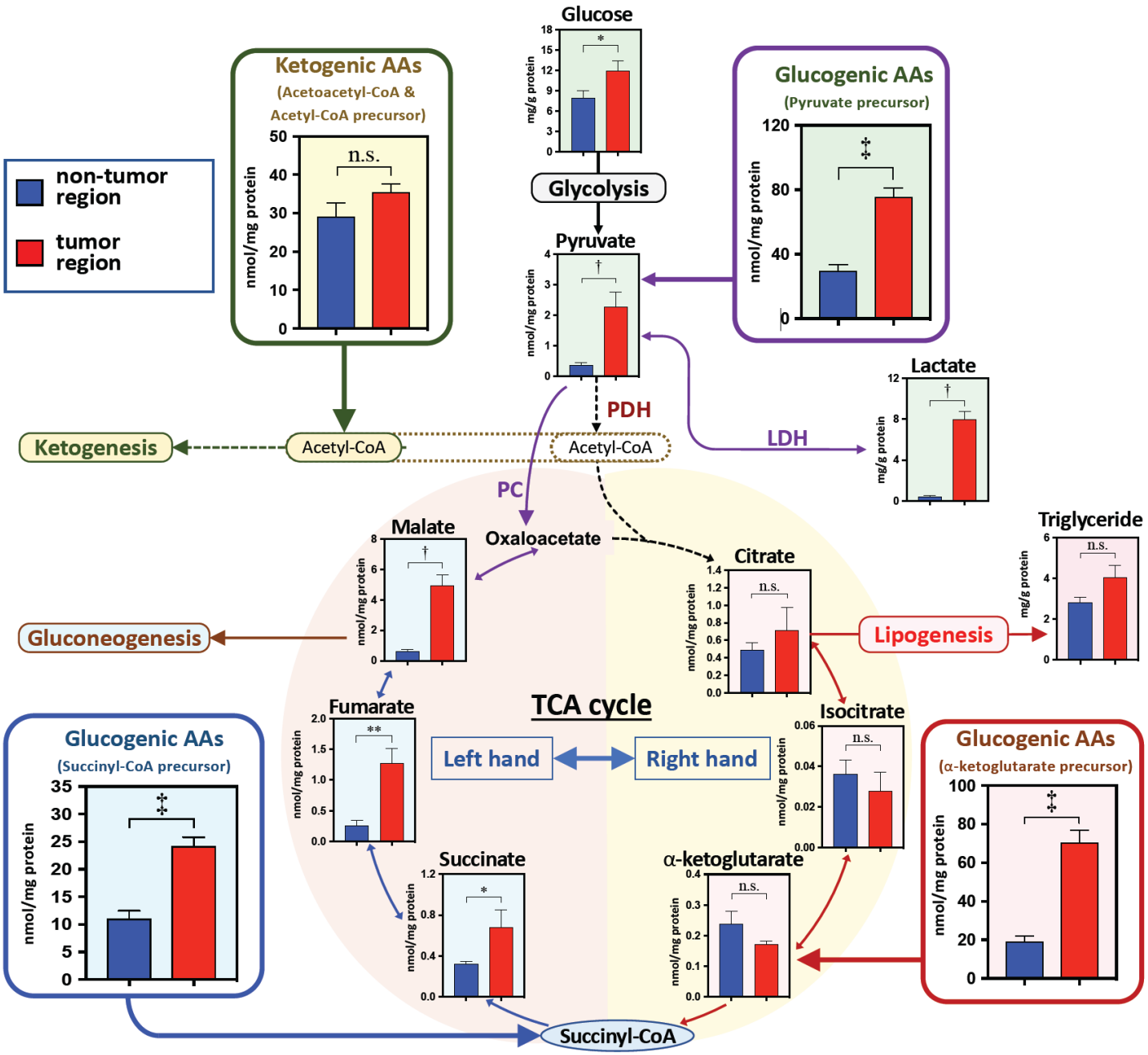
non-tumor region
tumor region
Ketogenic AAs
(Acetoacetyl-CoA & Acetyl-CoA precursor)
nmol/mg protein
n.s.
Glucose
mg/g protein
Glycolysis
Pyruvate
nmol/mg protein
Glucogenic AAs
(Pyruvate precursor)
nmol/mg protein
Lactate
mg/g protein
LDH
PDH
Ketogenesis
Acetyl-CoA
Acetyl-CoA
PC
Malate
nmol/mg protein
Oxaloacetate
Citrate
nmol/mg protein
n.s.
Triglyceride
mg/g protein
n.s.
Gluconeogenesis
Lipogenesis
TCA cycle
Left hand
Right hand
Fumarate
nmol/mg protein
Isocitrate
nmol/mg protein
n.s.
Glucogenic AAs
(Succinyl-CoA precursor)
nmol/mg protein
Succinate
nmol/mg protein
α-ketoglutarate
nmol/mg protein
n.s.
Glucogenic AAs
(α-ketoglutarate precursor)
nmol/mg protein
Succinyl-CoA

**Figure 2.** The metabolite levels in the amino acid (AA)-related metabolism in the nontumor and tumor regions. The sum of categorized AAs are presented by the metabolic precursors: pyruvate precursor (Ser + Gly + Thr + Ala + Tyr + Cys), acetyl-CoA precursor (Leu + Lys + Phe + Tyr + Ile + Trp), succinyl-CoA precursor (Val + Ile + Met + Thr), and α-ketoglutarate precursor (Glu + Gln + Arg + Pro). The concentrations of AAs and metabolites are presented as the tissue total protein level (nmol/mg total protein) and as the mean ± the standard error. **P*<0.05, ***P*<0.01, †*P*<0.001, and ‡*P*<0.0001 indicate the significant difference levels, analyzed using the paired Student's *t*-test. Abbreviation: AA, amino acid; LDH, lactate dehydrogenase; PC, pyruvate carboxylase.

**Table 2.** Glucose and amino acid concentrations in the nontumor and tumor regions with and without diabetes mellitus type II

| | Non-T2DM | | T2DM | | Two-way ANOVA analysis | | |
|---|---|---|---|---|---|---|---|
| | Nontumor | Tumor | Nontumor | Tumor | Tu | DM | Tu × DM |
| Glucose | 7.6±0.8 | 10.7±1.5 | 8.4±2.3 | 13.1±3.7 | n.s | n.s | n.s |
| *Pyruvate precursor* | | | | | | | |
| Ser | 5.4±1.1 | 10.2±0.6 | 5.0±0.6 | 9.3±1.5 | ** | n.s. | n.s. |
| Gly | 3.9±0.7 | 22.3±1.9 | 5.1±1.3 | 23.8±4.3 | ‡ | n.s. | n.s. |
| Thr[s] | 2.6±0.6 | 6.6±0.4 | 2.7±0.5 | 6.7±1.0 | † | n.s. | n.s. |
| Ala | 15.9±2.9 | 41.1±4.0 | 13.4±2.0 | 33.8±4.1 | ** | n.s. | n.s. |
| Trp[aa] | 0.4±0.1 | 0.6±0.1 | 0.4±0.1 | 0.9±0.1 | † | n.s. | n.s. |
| Cys | 0.4±0.0 | 0.3±0.1 | 0.4±0.1 | 0.6±0.3 | n.s. | n.s. | n.s. |
| *α-Ketoglutamate precursor* | | | | | | | |
| Gln | 5.1±1.1 | 17.3±2.2 | 5.4±1.1 | 13.9±3.4 | † | n.s. | n.s. |
| Glu | 2.8±0.8 | 42.6±5.6 | 4.5±1.6 | 32.1±9.4 | ‡ | n.s. | n.s. |
| Pro | 1.9±0.4 | 10.9±2.1 | 1.6±0.3 | 10.8±1.8 | † | n.s. | n.s. |
| Arg | 8.1±1.8 | 9.0±0.6 | 7.1±1.2 | 8.0±1.7 | n.s. | n.s. | n.s. |
| *Succinyl-CoA precursor* | | | | | | | |
| Met | 1.7±0.3 | 2.7±0.2 | 1.8±0.3 | 2.7±0.5 | * | n.s. | n.s. |
| Ile[a] | 1.7±0.3 | 3.5±0.3 | 1.5±0.2 | 3.9±0.6 | † | n.s. | n.s. |
| Val | 4.0±0.7 | 11.7±1.1 | 4.4±0.9 | 12.5±1.3 | ‡ | n.s. | n.s. |
| *Acetyl-CoA precursor* | | | | | | | |
| Leu | 6.1±1.2 | 7.8±0.5 | 5.8±0.8 | 8.3±1.1 | n.s. | n.s. | n.s. |
| *Acetoacetyl-CoA precursor* | | | | | | | |
| Lys | 13.8±2.3 | 17.4±1.5 | 12.6±2.1 | 15.6±3.2 | n.s. | n.s. | n.s. |
| Phe[f] | 3.2±0.6 | 4.4±0.4 | 3.3±0.8 | 4.4±0.7 | * | n.s. | n.s. |
| Tyr[f] | 3.7±0.8 | 4.8±0.4 | 4.3±1.1 | 4.7±0.7 | n.s. | n.s. | n.s. |

Footnote: Data are shown as the mean ± SE of mg/g protein and nmol/mg protein in glucose and AAs, respectively. Amino acids marked with *[a], [aa], [f], and [s] also* belong to the categories of the precursors of acetyl-CoA, acetoacetyl-CoA, fumarate, and succinyl-CoA, respectively. **P*<0.05, ***P*<0.01, †*P*<0.001, ‡*P*<0.0001, Abbreviations: n.s., no significant; T2DM, diabetes mellitus type II; Statistical differences were evaluated by two-way ANOVA analysis. Tu, ANOVA factor of tumor; DM, ANOVA factor of T2DM; Tu × DM, ANOVA factor of tumor and T2DM interaction.

factor-1α & β (HIF1α/β), and β-actin were significantly increased, compared to their levels in the nontumor region (**Figure 3C**).

## Discussion

The present study compared the profile of AAs and its related-metabolites in energy metabolism between the tumor and paired nontumor regions in lung tissues dissected from in patients with NSCLC. Based on a comparison of AAs categorized by their energy metabolic precursors, significantly increased glucogenic AAs levels and unchanged levels of ketogenic AAs were characteristics in the tumor region. In association with alterations of AA levels, characteristic differences existed in some metabolites in energy metabolism between the tumor and the paired nontumor regions. In particular, the metabolites in glycolysis and in the left-hand side of the TCA cycle (i.e., between succinyl-CoA and oxaloacetate) were significantly

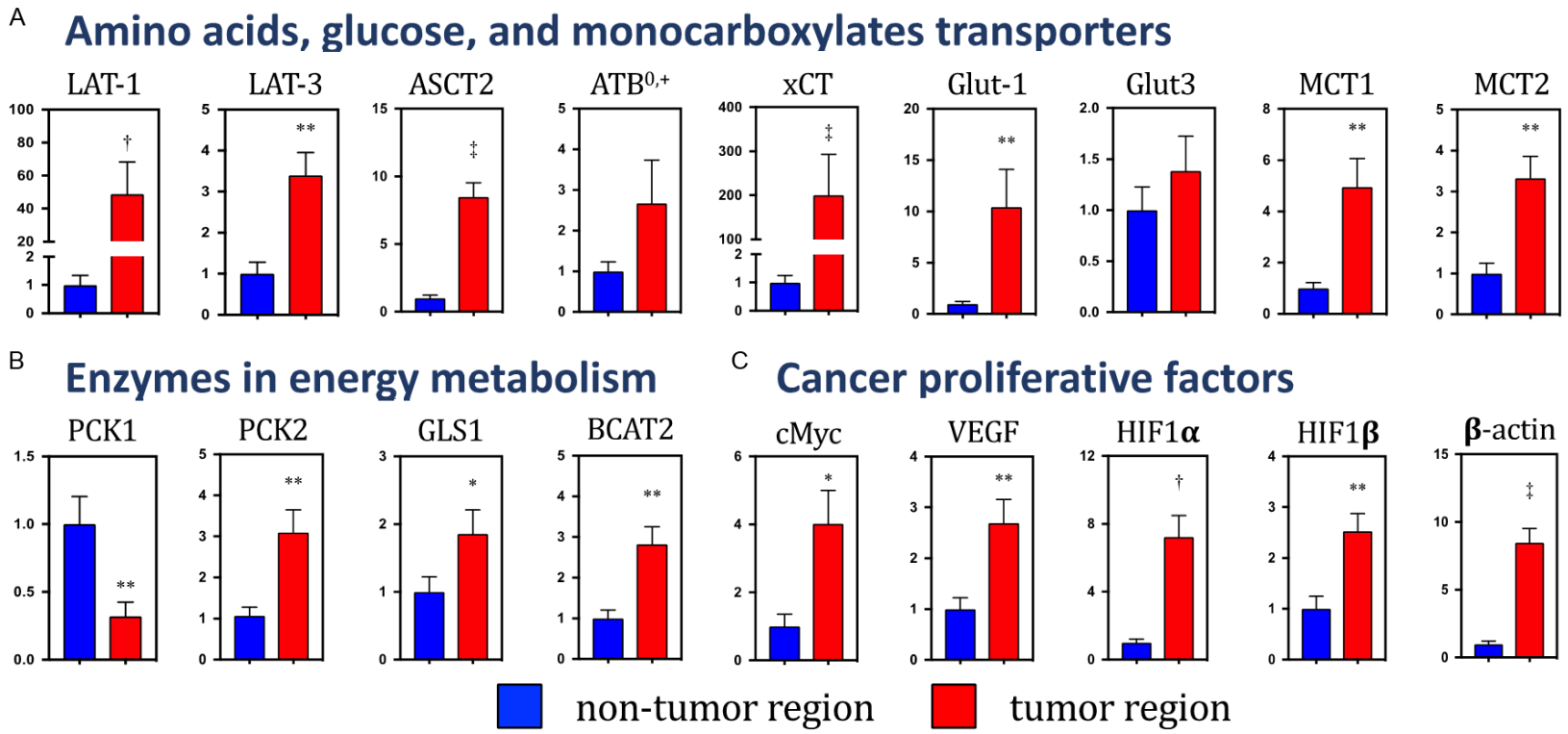


**Figure 3.** The mRNA expressions of the transporters, enzymes, and cancer proliferative factors in the nontumor and tumor regions. (A) Amino acids, glucose, and monocarboxylates transporters, (B) Energy metabolic enzymes involved in gluconeogenesis, glutaminolysis, and branched-chain amino acid catabolism. (C) Cancer proliferation factors. The mRNA expression level was standardized by using 18SrRNA. Data are presented as the mean ± the standard error of the relation to the expression level in the nontumor region. **P*<0.05, ***P*<0.01, †*P*<0.001, and ‡*P*<0.0001, compared to the nontumor region, and based on the paired Student's *t*-test. Abbreviation: 18SrRNA, 18S ribosomal RNA; ASCT2, system ASC transporter 2 (SLC1A5); $ATB^{0,+}$, amino acid transporter responsible for the activity of system $B^{0,+}$ (SLC6A14); BCAA, branched-chain amino acid; BCAT2, branched-chain amino acid transaminase-2; GLS1, glutaminase 1; Glut-1 & -3, glucose transporter type 1 & type 3 (SLC2A1 & SLC2A3); HIF-1α & β, hypoxia-inducible factor-1α & β; LAT-1 & -3, L-type amino acid transporter 1 & 3 (SLC7A5 & SLC43A1); MCT1 & 4, monocarboxylate transporter (SLC16A1 & SLC16A7); PCK1 &2, phosphoenolpyruvate carboxykinase 1 & 2; VEGFα, vascular endothelial growth factor α; xCT, system $x_c^-$ transporter-related protein (SLC7A11).

increased in the tumor region, whereas no differences existed between the two regions in the metabolites on the right-hand side of the TCA cycle (i.e., between citrate and α-ketoglutarate) between the two regions. These characteristics observed in lung cancer differ from those of previous evidence demonstrated that most AAs and their related metabolites were uniformly elevated in the tumor regions in stomach and colorectal cancers, compared to their levels in the paired nontumor regions [10]. Thus, the present study suggests that energy metabolism in lung cancer cells may be specific, compared with other types of cancers.

Carcinogenesis and diabetes mellitus have a strong association, based on energy metabolism, which comprises hyperinsulinemia, hyperglycemia, and fat-induced chronic inflammation, in various types of cancer [18]. In particular, the risk of cancer in the presence of T2DM has been proven for pancreatic, liver, breast, endometrium, bladder and kidney [19]. However, in the present study, no differences in the AA levels in the nontumor and tumor regions existed between patients with and without T2DM. The results suggested that energy metabolism, including AA involvement, in lung cancer may not be influenced by metabolic disorders in T2DM. Frasca *et al.* [20] reported that mRNA expression of the insulin receptor in the tumor region was not different from that of the paired nontumor region in lung cancer, whereas its expression was significantly higher in breast and colon cancers [20]. In addition, the potentially increased risk of lung cancer in T2DM patients treated with inhaled insulin is very low, based on long-time surveillance analysis [21]. Thus, the previous findings agree with the energy metabolism involved AAs is not strongly associated with T2DM in lung cancer cells.

In general, if the AA utilization for energy metabolism were increased under a low supply from extracellular circulation, then the AA contents should be reduced in the tumor region. On account that the blood supply is limited in the cancer cells, the origins of the increased AA contents in cancer cells were evaluated, based on the degradation of the extracellular matrix and the autophagic degradation of preexisting intracellular proteins [10].

Significant increases in HIF1α/β and VEGF mRNA levels associated with hypoxia were observed in the tumor region, compared to the paired nontumor region. Therefore, the tumor regions examined in the present study may be under similar gene regulations under low blood supply, as observed in other cancer types. However, blood supply to lung cancer cells, particularly NSCLC, is strongly suggested as sufficient because of the dual blood supply from the pulmonary and the bronchial artery system [12], unlike other cancer types. In addition, the mRNA expression of the examined main AA transporters was significantly increased in the tumor region, compared to their expression in the paired nontumor region. Therefore, significantly increased AA contents in the tumor region should be highly contributed by the increased AA uptakes from the extracellular circulation. In parallel, the idea of high AA utilization for energy production is supported by significant increases in the level of AA metabolites in the tumor region. In the tumor region, two AA metabolites in the succinyl-CoA product pathways-3HIB, an intermediate of valine, and 2HB, a byproduct from methionine and threonine [16]-were both significantly increased along with significant increases in the respective precursor AAs. The results support that the uptake from the blood supply and metabolism for energy production of AAs may be activated in the lung cancer cells.

In colon and stomach cancers, significantly lower levels of glucose and pyruvate, but significantly higher levels of lactate, were previously reported in the tumor region than in the corresponding normal counterparts; this finding indicated an association with the acceleration of glycolysis which is called the Warburg effect [10]. However, the present study demonstrated significant increases in lactate and in glucose and pyruvate in the tumor region. Louis *et al.* [22] have recently demonstrated that the plasma glucose level in patients with lung cancer was higher in nuclear magnetic resonance metabolomics evaluations.

In addition, the upregulation of Glut1, a major glucose transporter, has been well-documented in NSCLC [23]. The present study also observed significantly increased mRNA expression of Glut1 in the tumor region. Thus, the increased glucose level in the tumor region may be because of enhanced uptake through the dual blood supply system and may contribute

to the increase of pyruvate with its conversion from pyruvate precursor AAs. The increased lactate level was similarly in the tumor region observed in other cancer types [10].

However, Leithner *et al.* [24] demonstrated that lung cancers avidly uptake lactate and utilize it for gluconeogenesis as anaplerotic pathway via pyruvate carboxylation, after the conversion back to pyruvate. The enhanced extracellular uptake of lactate in lung cancer is supported by evidence of significantly increased mRNA expressions of MCT1 and MCT2 in the tumor region in the present study, and by cultured cancer cells and various cancer types, including lung cancer, in previous reports [25, 26]. The increased pyruvate derived from the glucogenic AAs and lactate in lung cancer would be a source for the gluconeogenesis pathway, which is generally activated for cell proliferation under low glucose conditions [27, 28].

In the NSCLC, the gluconeogenesis pathway may also be activated to meet the total metabolic demands of proliferating cancer cells, even if the glucose supply is sufficient. In the present study, the characteristic of significant increases in the levels of intermediates on the left-hand side of the TCA cycle suggested that gluconeogenesis was also activated in the tumor region. The metabolic directions are reversible, except for the rate-limiting reactions involving acetyl-CoA and succinyl-CoA; therefore, the increased levels of intermediates on the left-hand side may be because of the acceleration of metabolism due to oxaloacetate and succinyl-CoA. The reverse reaction from oxaloacetate occurs in gluconeogenesis, which is activated in most cancers, including lung cancer. The increased levels of intermediates on the left-hand side of the TCA cycle should be because of the activation of gluconeogenesis.

The previous studies have reported that the expression and activity of PC, in which carboxylates pyruvate derived from AAs and lactate to oxaloacetate, were upregulated in the patients with NSCLC [29, 30]. Furthermore, gluconeogenesis from oxaloacetate in the TCA cycle converted from AAs and other noncarbohydrate sources is enhanced in cancers through the upregulation of PEPCK, which is the rate-limiting enzyme of gluconeogenesis. In NSCLC, PEPCK2, which directly converts mitochondrial oxaloacetate to phosphoenolpyruvic acid without via malate, is highly expressed, but the cytoplasm isoform PEPCK1 [24, 31, 32] is not. The present study also confirmed significant mRNA upregulation and downregulation of PEPCK2 (PCK2) and PEPCK1 (PCK1), respectively, in the tumor region.

In addition, on the left-hand side of the TCA cycle, significant increases in intermediates such as succinate, fumarate, and malate in the tumor region were also possibly contributed to by the acceleration of succinyl-CoA production from the increased levels of glucogenic AAs because the levels of 3HIB and 2HB, and the mRNA expression of BCAT2 (i.e., the mitochondrial isoform of branched-chain transamidase) were significantly increased in the tumor region. However, some evidence exists regarding the evaluation of the succinyl-CoA production pathway from glucogenic AAs in cancer cells, whereas accumulated evidence exists for most cancers regarding the Warburg effect and glutaminolysis. Thus, the upregulation of succinyl-CoA production derived from glucogenic AAs may be a hallmark in lung cancers. More research is required regarding this issue.

However, the intermediates on the right-hand side of the TCA cycle were unchanged in the tumor region, whereas the α-ketoglutamate precursor AAs, including glutamate, glutamine, and proline were significantly increased. In cancer cells, the anaplerotic supply of α-ketoglutamate derived from glutamate is generally increased via glutaminolysis, which is an alternative anaplerotic supply system through the uptake of glutamine, the deamination of glutamine to glutamate, and the transamination to α-ketoglutarate. However, a previous metabolic flux study using $^{13}$C-labelled glucose reported that glutaminolysis was not activated and that gluconeogenesis through the PC pathway was instead enhanced in tumor tissue from patients with NSCLC, compared to healthy lung tissue [30]. The expression of GLS1, a key enzyme that converts glutamine to glutamate in the anaplerotic reaction, is increased in many cancer cells [6]. However, its unchanged expression in the tumor region has been reported in patients with NSCLC [30]. In the present study, the difference in gene expression between the two regions was significant but less than twofold. In addition, an unchanged glutamine level was observed in the tumor region compared to

the paired nontumor region, in colon and stomach cancers [10] in contrast to the present result. This finding contrasts with the present results. Glutamine is a nonessential AA, its metabolism is closely related to AA transporters [33]. The significant upregulation of ASCT2 and $ATB^{0,+}$, which are influx transporters of glutamine, are increased in breast cancer cells [34, 35]. Their levels were increased in the present study. By contrast, glutamine and its derived glutamate are exported out of the cells by LAT1, the antiporter for other AAs [6, 33] and xCT, the antiporter for cysteine [6, 33], respectively. In the present study, no differences existed in leucine and cysteine between the tumor and nontumor regions, whereas the mRNA expressions of LAT1 and xCT were markedly increased in the tumor region. However, significant increases in leucine and cysteine in the tumor region have been observed in colon and stomach cancers [10]. Therefore, specificities in the glutamine-related transporter systems through antiporters may exist in lung cancer.

The AA levels measured in the tissues results from dynamic balances between the uptake from extracellular fluids and the intracellular utilization for protein synthesis, gluconeogenesis, ketogenesis, and lipogenesis. The present study measured only the AA levels in the tissues; therefore, the direct dynamics of AA metabolism could not be clearly evaluated. The comparisons of the AAs and the intermediates of these AAs and energy metabolic pathways, including the glycolysis and TCA cycle should nevertheless support the evaluations of the AA-related metabolic differences between the tumor and nontumor regions in NSCLC.

In comparison to the nontumor regions in NSCLC, a significant increase in glucogenic AAs was the characteristics in the tumor region. In particular, higher levels of glucogenic AAs may be because of increased uptake from the extracellular supply by the upregulated AA transporters and may contribute to the acceleration of gluconeogenesis supported by the significant increases of the metabolic intermediates of AAs and on the left-hand side of the TCA cycle. Alterations in the AA-related metabolic balance were likely a specific adaptation of lung cancer to the energetic demands of the cancer under the tissue-specific blood supply system. These properties of energy metabolism associated with AAs in the tumor region may contribute to advancements in the early detection, prevention, and treatment of lung cancer.

## Acknowledgements

This study was supported by Kakenhi grant [18K08800].

## Disclosure of conflict of interest

None.

**Address correspondence to:** Dr. Kinya Furukawa, Department of Thoracic Surgery, Tokyo Medical University Ibaraki Medical Center, Ibaraki, Japan. Tel: +81-29-887-1161; E-mail: k-furu@tokyo-med.ac.jp

## References

[1] Dang CV and Semenza GL. Oncogenic alterations of metabolism. Trends Biochem Sci 1999; 24: 68-72.

[2] Warburg O. On the origin of cancer cells. Science 1956; 123: 309-314.

[3] Dang CV. Glutaminolysis: supplying carbon or nitrogen or both for cancer cells? Cell Cycle 2010; 9: 3884-3886.

[4] Zhang J, Pavlova NN and Thompson CB. Cancer cell metabolism: the essential role of the nonessential amino acid, glutamine. EMBO J 2017; 36: 1302-1315.

[5] Mazurek S and Eigenbrodt E. The tumor metabolome. Anticancer Res 2003; 23: 1149-1154.

[6] Altman BJ, Stine ZE and Dang CV. From Krebs to clinic: glutamine metabolism to cancer therapy. Nat Rev Cancer 2016; 16: 619-634.

[7] Ihata Y, Miyagi E, Numazaki R, Muramatsu T, Imaizumi A, Yamamoto H, Yamakado M, Okamoto N and Hirahara F. Amino acid profile index for early detection of endometrial cancer: verification as a novel diagnostic marker. Int J Clin Oncol 2014; 19: 364-372.

[8] Miyagi Y, Higashiyama M, Gochi A, Akaike M, Ishikawa T, Miura T, Saruki N, Bando E, Kimura H, Imamura F, Moriyama M, Ikeda I, Chiba A, Oshita F, Imaizumi A, Yamamoto H, Miyano H, Horimoto K, Tochikubo O, Mitsushima T, Yamakado M and Okamoto N. Plasma free amino acid profiling of five types of cancer patients and its application for early detection. PLoS One 2011; 6: e24143.

[9] Maeda J, Higashiyama M, Imaizumi A, Nakayama T, Yamamoto H, Daimon T, Yamakado M, Imamura F and Kodama K. Possibility of multivariate function composed of plasma amino acid profiles as a novel screening index for

non-small cell lung cancer: a case control study. BMC Cancer 2010; 10: 690.
[10] Hirayama A, Kami K, Sugimoto M, Sugawara M, Toki N, Onozuka H, Kinoshita T, Saito N, Ochiai A, Tomita M, Esumi H and Soga T. Quantitative metabolome profiling of colon and stomach cancer microenvironment by capillary electrophoresis time-of-flight mass spectrometry. Cancer Res 2009; 69: 4918-4925.
[11] Cascino A, Muscaritoli M, Cangiano C, Conversano L, Laviano A, Ariemma S, Meguid MM and Rossi Fanelli F. Plasma amino acid imbalance in patients with lung and breast cancer. Anticancer Res 1995; 15: 507-510.
[12] Milne EN. Circulation of primary and metastatic pulmonary neoplasms. A postmortem microarteriographic study. Am J Roentgenol Radium Ther Nucl Med 1967; 100: 603-619.
[13] Shimbo K, Oonuki T, Yahashi A, Hirayama K and Miyano H. Precolumn derivatization reagents for high-speed analysis of amines and amino acids in biological fluid using liquid chromatography/electrospray ionization tandem mass spectrometry. Rapid Commun Mass Spectrom 2009; 23: 1483-1492.
[14] Miyazaki T, Nagasaka H, Komatsu H, Inui A, Morioka I, Tsukahara H, Kaji S, Hirayama S, Miida T, Kondou H, Ihara K, Yagi M, Kizaki Z, Bessho K, Kodama T, Iijima K, Yorifuji T, Matsuzaki Y and Honda A. Serum amino acid profiling in citrin-deficient children exhibiting normal liver function during the apparently healthy period. JIMD Rep 2019; 43: 53-61.
[15] Nagasaka H, Komatsu H, Inui A, Nakacho M, Morioka I, Tsukahara H, Kaji S, Hirayama S, Miida T, Kondou H, Ihara K, Yagi M, Kizaki Z, Bessho K, Kodama T, Iijima K, Saheki T, Yorifuji T and Honda A. Circulating tricarboxylic acid cycle metabolite levels in citrin-deficient children with metabolic adaptation, with and without sodium pyruvate treatment. Mol Genet Metab 2017; 120: 207-212.
[16] Miyazaki T, Honda A, Ikegami T, Iwamoto J, Monma T, Hirayama T, Saito Y, Yamashita K and Matsuzaki Y. Simultaneous quantification of salivary 3-hydroxybutyrate, 3-hydroxyisobutyrate, 3-hydroxy-3-methylbutyrate, and 2-hydroxybutyrate as possible markers of amino acid and fatty acid catabolic pathways by LC-ESI-MS/MS. Springerplus 2015; 4: 494.
[17] Shiina I, Ibuka R and Kubota M. A new condensation reaction for the synthesis of carboxylic esters from nearly equimolar amounts of carboxylic acids and alcohols using 2-methyl-6-nitrobenzoic anhydride. Chem Lett 2002; 3: 286-287.
[18] Wojciechowska J, Krajewski W, Bolanowski M, Krecicki T and Zatonski T. Diabetes and cancer: a review of current knowledge. Exp Clin Endocrinol Diabetes 2016; 124: 263-275.
[19] Vigneri P, Frasca F, Sciacca L, Pandini G and Vigneri R. Diabetes and cancer. Endocr Relat Cancer 2009; 16: 1103-1123.
[20] Frasca F, Pandini G, Scalia P, Sciacca L, Mineo R, Costantino A, Goldfine ID, Belfiore A and Vigneri R. Insulin receptor isoform A, a newly recognized, high-affinity insulin-like growth factor II receptor in fetal and cancer cells. Mol Cell Biol 1999; 19: 3278-3288.
[21] Mitri J and Pittas AG. Inhaled insulin--what went wrong. Nat Clin Pract Endocrinol Metab 2009; 5: 24-25.
[22] Louis E, Adriaensens P, Guedens W, Bigirumurame T, Baeten K, Vanhove K, Vandeurzen K, Darquennes K, Vansteenkiste J, Dooms C, Shkedy Z, Mesotten L and Thomeer M. Detection of lung cancer through metabolic changes measured in blood plasma. J Thorac Oncol 2016; 11: 516-523.
[23] Brown RS, Leung JY, Kison PV, Zasadny KR, Flint A and Wahl RL. Glucose transporters and FDG uptake in untreated primary human non-small cell lung cancer. J Nucl Med 1999; 40: 556-565.
[24] Vincent EE, Sergushichev A, Griss T, Gingras MC, Samborska B, Ntimbane T, Coelho PP, Blagih J, Raissi TC, Choiniere L, Bridon G, Loginicheva E, Flynn BR, Thomas EC, Tavare JM, Avizonis D, Pause A, Elder DJ, Artyomov MN and Jones RG. Mitochondrial phosphoenolpyruvate carboxykinase regulates metabolic adaptation and enables glucose-independent tumor growth. Mol Cell 2015; 60: 195-207.
[25] Payen VL, Mina E, Van Hee VF, Porporato PE and Sonveaux P. Monocarboxylate transporters in cancer. Mol Metab 2020; 33: 48-66.
[26] Pinheiro C, Reis RM, Ricardo S, Longatto-Filho A, Schmitt F and Baltazar F. Expression of monocarboxylate transporters 1, 2, and 4 in human tumours and their association with CD147 and CD44. J Biomed Biotechnol 2010; 2010: 427694.
[27] Leithner K, Hrzenjak A and Olschewski H. Gluconeogenesis in cancer: door wide open. Proc Natl Acad Sci U S A 2014; 111: E4394.
[28] Balsa-Martinez E and Puigserver P. Cancer cells hijack gluconeogenic enzymes to fuel cell growth. Mol Cell 2015; 60: 509-511.
[29] Fan TW, Lane AN, Higashi RM, Farag MA, Gao H, Bousamra M and Miller DM. Altered regulation of metabolic pathways in human lung cancer discerned by (13)C stable isotope-resolved metabolomics (SIRM). Mol Cancer 2009; 8: 41.
[30] Sellers K, Fox MP, Bousamra M 2nd, Slone SP, Higashi RM, Miller DM, Wang Y, Yan J, Yuneva MO, Deshpande R, Lane AN and Fan TW. Pyruvate carboxylase is critical for non-small-cell lung cancer proliferation. J Clin Invest 2015; 125: 687-698.

[31] Leithner K, Hrzenjak A, Trotzmuller M, Moustafa T, Kofeler HC, Wohlkoenig C, Stacher E, Lindenmann J, Harris AL, Olschewski A and Olschewski H. PCK2 activation mediates an adaptive response to glucose depletion in lung cancer. Oncogene 2015; 34: 1044-1050.

[32] Zhang P, Tu B, Wang H, Cao Z, Tang M, Zhang C, Gu B, Li Z, Wang L, Yang Y, Zhao Y, Wang H, Luo J, Deng CX, Gao B, Roeder RG and Zhu WG. Tumor suppressor p53 cooperates with SIRT6 to regulate gluconeogenesis by promoting FoxO1 nuclear exclusion. Proc Natl Acad Sci U S A 2014; 111: 10684-10689.

[33] Kandasamy P, Gyimesi G, Kanai Y and Hediger MA. Amino acid transporters revisited: new views in health and disease. Trends Biochem Sci 2018; 43: 752-789.

[34] van Geldermalsen M, Wang Q, Nagarajah R, Marshall AD, Thoeng A, Gao D, Ritchie W, Feng Y, Bailey CG, Deng N, Harvey K, Beith JM, Selinger CI, O'Toole SA, Rasko JE and Holst J. ASCT2/SLC1A5 controls glutamine uptake and tumour growth in triple-negative basal-like breast cancer. Oncogene 2016; 35: 3201-3208.

[35] Karunakaran S, Ramachandran S, Coothankandaswamy V, Elangovan S, Babu E, Periyasamy-Thandavan S, Gurav A, Gnanaprakasam JP, Singh N, Schoenlein PV, Prasad PD, Thangaraju M and Ganapathy V. SLC6A14 (ATB0,+) protein, a highly concentrative and broad specific amino acid transporter, is a novel and effective drug target for treatment of estrogen receptor-positive breast cancer. J Biol Chem 2011; 286: 31830-31838.